International Journal of Nanomedicine

Dovepress
open access to scientific and medical research

Open Access Full Text Article

ORIGINAL RESEARCH

Angiopep-2-conjugated poly(ethylene glycol)-*co*-poly(ε-caprolactone) polymersomes for dual-targeting drug delivery to glioma in rats

This article was published in the following Dove Press journal:
International Journal of Nanomedicine
16 March 2017
Number of times this article has been viewed

Fei Lu[1,2]
Zhiyong Pang[2,3]
Jingjing Zhao[2]
Kai Jin[4]
Haichun Li[2]
Qiang Pang[2]
Long Zhang[2]
Zhiqing Pang[2]

[1]Department of Pharmacy, Xianju People's Hospital, Xianju, Zhejiang, [2]Department of Pharmaceutics, Key Laboratory of Smart Drug Delivery, Ministry of Education and PLA, School of Pharmacy, Fudan University, Shanghai, [3]Chongyang Center for Disease Control and Prevention, Xianning, Hubei, [4]School of Life Science, Fudan University, Shanghai, People's Republic of China

Abstract: The blood–brain barrier is a formidable obstacle for glioma chemotherapy due to its compact structure and drug efflux ability. In this study, a dual-targeting drug delivery system involving Angiopep-2-conjugated biodegradable polymersomes loaded with doxorubicin (Ang-PS-DOX) was developed to exploit transport by the low-density lipoprotein receptor-related protein 1 (LRP1), which is overexpressed in both blood–brain barrier and glioma cells. The polymersomes (PS) were prepared using a thin-film hydration method. The PS were loaded with doxorubicin using the pH gradient method (Ang-PS-DOX). The resulting PS were uniformly spherical, with diameters of ~135 nm and with ~159.9 Angiopep-2 molecules on the surface of each PS. The drug-loading capacity and the encapsulation efficiency for doxorubicin were 7.94%±0.17% and 95.0%±1.6%, respectively. Permeability tests demonstrated that the proton diffusion coefficient across the PS membrane was far slower than that across the liposome membrane, and the common logarithm value was linearly dependent on the dioxane content in the external phase. Compared with PS-DOX, Ang-PS-DOX demonstrated significantly higher cellular uptake and stronger cytotoxicity in C6 cells. In vivo pharmacokinetics and brain distribution experiments revealed that Ang-PS-DOX achieved a more extensive distribution and more abundant accumulation in glioma cells than PS-DOX. Moreover, the survival time of glioma-bearing rats treated with Ang-PS-DOX was significantly prolonged compared with those treated with PS-DOX or a solution of free doxorubicin. These results suggested that Ang-PS-DOX can target glioma cells and enhance chemotherapeutic efficacy.

Keywords: Angiopep-2, dual targeting, biodegradable polymersomes, doxorubicin, glioma treatment

Introduction

Glioma accounts for ~80% of central nervous system tumors and is the most common primary malignant brain tumor in adults.[1,2] Glioma is associated with a poor prognosis; the median survival of glioma patients who undergo aggressive treatment is <14.4 months and the 5-year survival rate is <5%.[1,3,4] Surgery cannot completely remove the tumor tissues completely because of the diffuse invasion of tumor cells.[5] For this reason, adjunctive radiotherapy and chemotherapy are essential. However, the blood–brain barrier (BBB) prevents most therapeutic agents from entering the brain parenchyma.[6] Another obstacle associated with chemotherapy is promoting drug accumulation in the tumor sites while preventing therapeutic agents from accessing surrounding healthy tissues.[7]

Many strategies based on different mechanisms have been proposed to solve these problems, including osmotic BBB disruption,[8] bradykinin receptor-mediated BBB opening,[9]

Correspondence: Zhiqing Pang
Department of Pharmaceutics, Key Laboratory of Smart Drug Delivery, Ministry of Education and PLA, School of Pharmacy, Fudan University, 826 N Zhangheng Road, Shanghai 201203, People's Republic of China
Tel +86 21 5198 0069
Email zqpang@fudan.edu.cn

submit your manuscript | www.dovepress.com
Dovepress
http://dx.doi.org/10.2147/IJN.S123422

inhibition of drug efflux transporters,[10] receptor-mediated transport systems,[11,12] and circumvention of the BBB.[13,14] Among these strategies, noninvasive receptor-mediated transport system has shown promise for clinical application.

Low-density lipoprotein receptor-related protein 1 (LRP1) is highly expressed on the endothelial cells of brain capillaries[15–17] and has been utilized to deliver potential therapeutic agents across the BBB to the central nervous system. LRP1 is also overexpressed in glioma and brain metastases from lung, skin, and breast cancers,[18] but weakly expressed in normal brain parenchyma.[15,19,20] This feature makes LRP1 a potential target for glioma therapy. Angiopep-2, a peptide derived from the Kunitz domains of aprotinin, can specifically bind LRP1.[18] Importantly, Angiopep-2 has higher transcytosis and parenchymal accumulation than transferrin and lactoferrin, which are commonly used for brain-targeting drug delivery systems.[18,19,21–23] All of these characteristics make Angiopep-2 a promising candidate for LRP1-mediated dual-targeting drug delivery to glioma tumors.

Doxorubicin (DOX), an anthracycline ring antibiotic, exerts antitumor activity by interfering with DNA synthesis.[24] It has been extensively used for the treatment of peripheral tumors; however, there is still a huge gap for the clinical application of DOX in brain tumor therapy because of its rapid clearance and poor delivery across the BBB. To solve this problem, DOX has been encapsulated or conjugated with various nanocarriers to utilize the enhanced permeation and retention (EPR) effect of tumor cells.[25] Several specific ligands were connected to nanocarriers to achieve better brain distribution.[20] Among these, self-assembled biodegradable polymersomes (PS) made of amphiphilic block copolymers[26] have attracted great interest due to their stable structure, tunable membrane, broad range of drug-encapsulating capacity, and long circulatory half-life.[27] In view of the aforementioned advantages, Angiopep-2-conjugated biodegradable PS (Ang-PS) loaded with DOX (Ang-PS-DOX) might improve DOX pharmacokinetics, enhance glioma cell drug delivery, and boost chemotherapy efficacy.

The objective of the present study was to assess the potential of Ang-PS, a dual-targeting glioma drug delivery system for the treatment of glioma. The PS were prepared with a thin-film hydration method. The structure and the shape were visualized under cryo-transmission electron microscope (Cryo-TEM) and transmission electron microscope (TEM), respectively. Proton diffusion across the PS membrane was investigated to assess tunable membrane permeability. DOX was loaded by the pH gradient method. Size, zeta potential, drug loading, and drug release of Ang-PS-DOX were determined. Cellular uptake and cytotoxicity assay were investigated using C6 cells. In vivo pharmacokinetics and brain tumor distribution experiments were performed in glioma-bearing rats to reveal the dual-targeting delivery property of Ang-PS-DOX. Finally, survival experiments were conducted to evaluate the antiglioma efficacy of Ang-PS-DOX.

Materials and methods

Materials and animals

Methoxypolyethylene glycol (MPEG, molecular weight [MW] 3,000 Da) was purchased from PegBio (Suzhou, People's Republic of China). Maleimide-polyethylene glycol (PEG; MW 3,400 Da) was ordered from Laysan Bio (Arab, AL, USA). Methoxypoly(ethylene glycol)-*b*-polycaprolactone (3k–16k Da, MPEG3k-PCL16k) or maleimide-PEG3.4k-PCL16k diblock copolymers were synthesized by ring-opening polymerization of ε-caprolactone using MPEG or maleimide-PEG as the initiator as previously described.[28] Angiopep-2 (CTFFYGGSRGKRNNFKTKRY) was ordered from Chinese Peptide (Huangzhou, People's Republic of China). DOX and daunorubicin were purchased from Beijing Huafeng United Technology (Beijing, People's Republic of China). 8-Hydroxypyrene-1,3,6-trisulfonic acid trisodium salt (HTPS) was from Sigma-Aldrich Co. (St Louis, MO, USA). 4′,6-Diamidino-2-phenylindole, dihydrochloride (DAPI) was from Beyotime Biotechnology (Shanghai, People's Republic of China). The C6 and C6-green fluorescent protein (GFP) cell lines were bought from Shanghai SBO Medical Biotechnology (Shanghai, People's Republic of China). Dulbecco's Modified Eagle's Medium (high-glucose) cell culture medium, plastic cell culture dishes, and plates were purchased from Corning Incorporated (Corning, NY, USA). Fetal bovine serum was obtained from Gibco/Thermo Fisher Scientific (Waltham, MA, USA). Trypsin–ethylenediaminetetraacetic acid and penicillin–streptomycin solution were provided by Thermo Fisher Scientific. Double-distilled water was purified using a Millipore Simplicity System (EMD Millipore, Billerica, MA, USA). All other chemical reagents were of analytical or chromatographic pure grade and were purchased from Sinopharm Chemical Reagent (Shanghai, People's Republic of China).

Male Wistar strain rats (weighing 200–230 g) were obtained from Shanghai SLAC Laboratory Animal Co. Ltd. (Shanghai, People's Republic of China), maintained under standard housing conditions, and provided with sufficient food and water. The animals involved in this

study were treated according to the protocols evaluated and approved by the ethical committee of Fudan University. All animal experiments were performed following national regulations for the administration of affairs concerning experimental animals.

Biodegradable PS preparation

Biodegradable PS were prepared with a blend of MPEG-PCL and maleimide-PEG-PCL by a thin-film hydration method. Briefly, 20 mg MPEG3k-PCL16k and 2 mg maleimide-PEG3.4k-PCL16k were dissolved in 10 mL dichloromethane. The dichloromethane was removed by rotary evaporation for 2 h at 40°C with a ZX-98 rotary evaporator (Shanghai Institute of Organic Chemistry, Shanghai, People's Republic of China). The thin polymer film formed in a round-bottom flask was hydrated with 4 mL 0.2 M citrate buffer (pH 4.0) at 60°C to obtain the PS suspension. Liposomes were prepared with the same methods, except that 15 mg egg phosphatidylcholine and 5 mg cholesterol were dissolved in 10 mL dichloromethane. Afterward, the liposomes were sonicated (200 W, 2 seconds for 15 times) by a probe sonicator (Scientz Biotechnology Co. Ltd., Ningbo, People's Republic of China) to yield 110 nm liposomes.

DOX was actively entrapped in PS by a pH gradient method.[29,30] In brief, 2 mg DOX was added to the PS suspension and the pH value was adjusted to 7.4 using 1 M Na_2CO_3. Then, dioxane, a plasticizer of the PS membrane used to increase the permeability to facilitate active loading of DOX,[31] was added to the PS suspension and incubated for 1 h in the dark at 40°C. Ultrafiltration was performed to remove dioxane and unentrapped DOX and concentrate DOX-loaded PS (PS-DOX).

Ang-PS preparation

PS were incubated with Angiopep-2 in 4-(2-hydroxyethyl)-1-piperazineethanesulfonic acid buffer (pH 7.0) and stirred mildly for 8 h under pure nitrogen conditions at room temperature. In this process, maleimide groups at the surface specifically reacted with the thiol groups of Angiopep-2, and the molar ratio of maleimide to Angiopep-2 was 3:1.[32] Free Angiopep-2 was removed by centrifugation at 21,000× *g* for 40 min at 4°C. The amount of Angiopep-2 in the supernatant was quantified by the micro-bicinchoninic acid method,[33] where absorbance was measured at 562 nm using a spectrophotometer (Molecular Devices LLC, Sunnyvale, CA, USA). The coupling efficiency was obtained by dividing the amount of Angiopep-2 on Ang-PS by the weight of the Angiopep-2 input. The surface density of Angiopep-2 on PS was determined by dividing the number of Angiopep-2 molecules by the calculated average number of PS using methods described by Olivier et al.[32] DOX-loaded Angiopep-2-conjugated PS (Ang-PS-DOX) were prepared using the same procedure by linking Angiopep-2 to the surface of PS-DOX.

Blank PS characterization

PS formation was visualized by Cryo-TEM (JEOL, Tokyo, Japan).[34] PS morphology and size were observed by TEM (JEM-1230, JEOL) after negative staining with 1% uranyl acetate solution. The average diameters and zeta potential of PS and Ang-PS dispersed in 0.001 M NaCl solution were determined by dynamic light scattering using a Nano ZS Zetasizer (Malvern Instruments, Malvern, UK).

PS permeability

PS permeability plays a vital role in the drug-loading process and storage stability.[35,36] In the present study, the proton (H^+) was selected for permeability determination of PS due to its small size, strong polarity, and weak permeability across PS membranes. Proton efflux was determined by measuring the pH changes of the solution outside PS with HPTS acting as a pH-sensitive fluorescence probe.[31] First, the correlation between fluorescence intensity ratios of HPTS at 403 and 454 nm (I_{403}/I_{454} or I_{454}/I_{403}) and the pH value of the exterior aqueous phase was determined. In brief, the fluorescence excitation spectra of HPTS solution (2.5 μmol/L) at various pH values were scanned (from 350 to 500 nm, Em =509 nm). The fluorescence intensity ratios vs pH values were regressed with the Boltzmann function. Second, to determine the proton diffusion rate across the PS membrane with different dioxane contents, proton-encapsulated PS were prepared as described above and eluted by a sepharose cross-linked 4B column with NaCl solution (pH 9.8). Then the PS solution was divided into four aliquots, and 0%, 10%, 20%, or 40% (V/V) dioxane was added. Next, HPTS was added to each aliquot, and the HPTS concentrations in the external aqueous phase PS were all 2.5 μmol/L. At preset time points, the fluorescence excitation spectra of PS solution were scanned (from 350 to 500 nm, Em =509 nm). The proton concentrations derived from the intensity ratios (I_{403}/I_{454} or I_{454}/I_{403}) at different time points were calculated, and the curves of proton concentrations against the square root of diffusion time t were plotted. The diffusion coefficient (D^*) of the protons across the PS membrane was calculated according to the following formula and compared with liposomes: $\frac{dC_{out}}{dt^{1/2}} \approx C_{in}\sqrt{\frac{NV_{in}AD^*}{V_{out}L}}$, where C_{out} is the proton concentration in the external aqueous phase, t is the diffusion time,

A is the average surface area of PS, N is the number of PS per unit volume, L is the PS membrane thickness, and V_{in} and V_{out} are the internal and external volumes, respectively.[31]

Ang-PS-DOX characterization

The average diameters and zeta potential of PS-DOX and Ang-PS-DOX were determined as those of blank PS. The drug-loading capacity (DLC) and the encapsulation efficiency (EE) of DOX-loaded PS were both determined using a high-performance liquid chromatography (HPLC) method. Briefly, DOX-loaded PS were disrupted with a ninefold volume of acetonitrile, and water was added to extract DOX. After centrifugation, the DOX concentration in the supernatant was analyzed by an HPLC system (Shimadzu Scientific Instrument Inc., Kyoto, Japan) equipped with a fluorescence detector (model RF-10AXL; excitation wavelength (Ex) =480 nm, emission wavelength (Em) =550 nm) and a Dikma Diamonsil® C18 (5 mm, 200×4.6 mm) column at 35°C. The mobile phase consisted of potassium dihydrogen phosphate, acetonitrile, and glacial acetic acid (145:55:0.6, v/v) with pH 3.0 at a flow rate of 1.2 mL/min. The sample injection volume was 20 µL. The DLC and EE of DOX in the PS were calculated as follows:

$$\text{DLC}\ (\%) = \frac{\text{DOX encapsulated}}{\text{Total PS}} \times 100\%;$$

$$\text{EE}\ (\%) = \frac{\text{DOX encapsulated}}{\text{DOX imput}} \times 100\%$$

In vitro Ang-PS-DOX release

The in vitro cumulative release profiles of DOX from Ang-PS-DOX in different media were determined as described previously.[37] In brief, 1.0 mL of Ang-PS-DOX was transferred into a dialysis bag (MW cutoff 14 kDa) and submerged in 10 mL of 0.01 M phosphate-buffered saline (PBS, pH 4.0), 0.01 M PBS (pH 7.4), or 10% fetal bovine serum in 0.01 M PBS at 37°C with slow stirring. At preset time points, samples were withdrawn and an equal volume of fresh release medium was immediately supplemented. The amount of DOX released was determined by the HPLC method described above.

Cellular uptake of Ang-PS-DOX

To investigate the cellular uptake of Ang-PS-DOX, C6 cells were seeded onto 24-well plates at a density of 10^5 cells per well and cultured for 24 h. The cells were exposed to PS-DOX, Ang-PS-DOX, or free DOX solution for 4 h at 37°C. The DOX concentration of each formulation was 4 µg/mL per well. For fluorescence imaging, these cells were fixed with 4% paraformaldehyde, stained with 1 µg/mL DAPI at room temperature, washed in PBS three times, and then visualized under a fluorescence microscope (IX71; Olympus Corporation, Tokyo, Japan). To quantify the cell fluorescence intensity, the cells were digested with trypsin, harvested by centrifugation, suspended in PBS, and subjected to a fluorescence-activated cell sorting Aria cell sorter (BD Biosciences, Franklin Lakes, NJ, USA).

In vitro cytotoxicity of DOX-loaded PS against C6 cells

The in vitro cytotoxicity of DOX-loaded PS against C6 cells was assayed with 3-(4,5-dimethylthiazol-2-yl)-2,5-diphenyltetrazolium bromide (MTT) assays. Briefly, C6 cells were planted onto 96-well plates at a density of 10^4 cells per well and incubated for 24 h, followed by exposure to free DOX, PS-DOX, or Ang-PS-DOX with a series of DOX concentrations for another 24 h at 37°C. The cytotoxicities of these formulations were determined by the MTT assay according to the routine protocol, and the absorbance was measured by a microplate reader (Bio-TEK, Winooski, VT, USA) at a wavelength of 570 nm. The half-maximal inhibitory concentration (IC_{50}) values of PS-DOX and Ang-PO-DOX against C6 cells were analyzed by GraphPad Prism v6.02 software (GraphPad Inc., La Jolla, CA, USA).

Tumor implantation

Glioma-bearing rat models were established by intracranial injection of C6 cells into the striatum as described previously.[38] In brief, rats were subjected to the stereotaxic instrument after intraperitoneal anesthetization with chloral hydrate (0.4 g/kg). Then, ~3×10^5 C6 cells (in 5 µL sterile PBS) were injected into the caudate nucleus region, which was 1 mm posterior and 2 mm right to the bregma and 4.5 mm beneath the exposed dura mater. The hole in the skull was sealed with sterilized bone wax, and the scalp incision was sutured.

Pharmacokinetics and brain delivery of DOX-loaded PS

In vivo pharmacokinetics and brain delivery of different DOX formulations were investigated as previously described.[39] Briefly, 12 days after tumor implantation, glioma-bearing rats were randomly divided into three groups and treated with DOX solution, PS-DOX, or Ang-PS-DOX correspondingly by intravenous (i.v.) injection. The DOX dosage for each group was 5 mg/kg. For pharmacokinetics studies, blood samples were collected by cheek-pouch (submandibular) puncture at each set time point. At 24 h after i.v. injection,

the animals were sacrificed followed by heart perfusion with saline, and the cerebral cortex, left striatum, and right striatum (tumor tissue) together with other organ samples were carefully harvested and immediately washed with cold saline. DOX concentrations in the tissues and plasma were determined by the HPLC method. Briefly, samples were homogenized with a threefold volume of PBS in an ice bath. Ten microliters of daunorubicin (10 μg/mL), acting as an internal standard, was added to the tissue homogenate. After that, the samples were extracted with 2 mL chloroform:methanol (4:1, v/v), followed by an intense 2 min vortex. After a 10 min centrifugation at 4,000× *g*, the supernatant was transferred and evaporated with a gentle nitrogen stream at 40°C. The residue was dissolved in 200 μL methanol, and 20 μL was injected into the HPLC system as described above. For blood plasma samples, the extraction and chromatographic analysis processes were similar to that of the tissue, except that a threefold volume of PBS was not added. For data analysis, the percentage of injected dose (%ID) per milliliter of plasma, brain uptake, and organ biodistribution (expressed as %ID per gram of tissue) were calculated as previously described.[38,40] The pharmacokinetics parameters including area under the concentration–time curve (AUC_{0-t}), mean residence time (MRT_{0-t}), and clearance (Cl) were calculated by DAS 3.0 software (Professional Committee of Pharmacometrics of China, Beijing, People's Republic of China).

Distribution of DOX-loaded PS in glioma

Glioma-bearing rats were established as described above. Twelve days after C6-GFP cell inoculation, PS-DOX or Ang-PS-DOX was injected into the tail veins of glioma-bearing rats at the DOX dosage of 5 mg/kg. The rats were perfused with PBS (0.01 M, pH 7.4) and 4% paraformaldehyde 24 h later. Brains were harvested and fixed in 4% paraformaldehyde for 24 h, followed by sequential dehydration with 15% and 30% sucrose solutions. After that, the brains were frozen in Tissue-Tek Optimum Cutting Temperature Compound (Sakura Finetek USA, Torrance, CA, USA) at −80°C and sectioned into 10 μm slices. The fluorescence distribution of DOX-loaded PS in brain tumor slices was imaged under a fluorescence microscope (DMI 4000B; Leica Microsystems, Wetzlar, Germany) after being stained with DAPI. The overlay of red DOX-loaded PS with GFP-labeled glioma cells was analyzed by ImageJ 1.48 software (National Institutes of Health, Bethesda, MD, USA).

Antiglioma efficacy

The orthotropic glioma-bearing rat models were established as described above. Forty rats were randomly divided into four groups and treated with 100 μL saline, free DOX solution, PS-DOX, or Ang-PS-DOX through the tail vein (DOX dosage of 1.5 mg/kg) at 5, 8, 11, and 14 days after C6 cell inoculation. The body weights of tumor-bearing rats were measured every 2 days and analyzed by GraphPad Prism v6.02. The survival times of animals were recorded, and the data were processed by Kaplan–Meier survival log-rank analysis to evaluate the antiglioma efficacy of different DOX formulations.

Statistical analysis

Unpaired Student's *t*-tests were used to assess statistically significant differences between two groups, and one-way analyses of variance were performed used for multiple-group analyses. Data are expressed as mean ± standard deviation (SD), and $P<0.05$ was considered statistically significant.

Results and discussion

Characterization of blank PS

The Cryo-TEM and TEM imaging results indicated that the assembled blank PS were uniformly round and vesicle-like shaped with a diameter of ~105 nm (Figure 1A and B). The membrane thickness was homogeneous, with a measured width

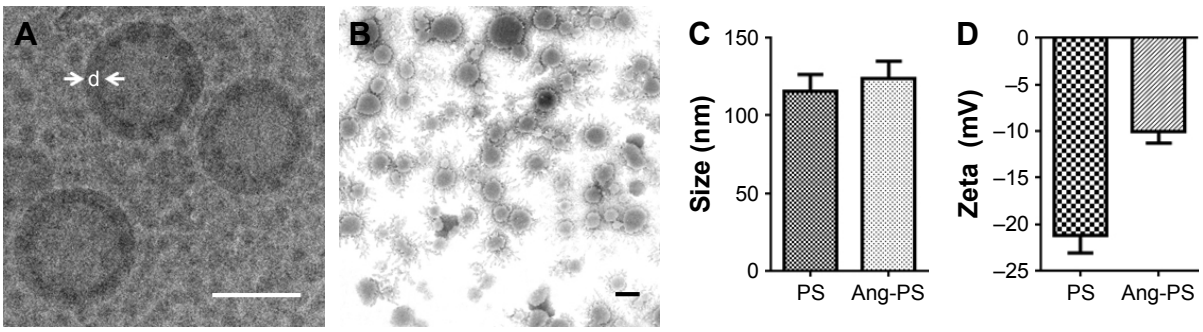

Figure 1 Characterization of blank PS.
Notes: (**A**) Cryo-TEM image, (**B**) TEM image, (**C**) size, and (**D**) zeta potential of PS and Ang-PS. Bar =100 nm.
Abbreviations: Ang-PS, Angiopep-2-conjugated biodegradable polymersomes; PS, polymersomes; TEM, transmission electron microscope.

d of ~16 nm. The PS diameter obtained with the dynamic light scattering method was similar with those observed in Cryo-TEM and TEM images (Figure 1C). Conjugation of Angiopep-2 to blank PS slightly increased the size from 115.2±11.2 to 123.4±11.5 nm, but significantly increased the zeta potential from −21.2±1.9 to −10.1±1.2 mV (Figure 1D). The coupling efficiency of Angiopep-2 to PS was around 31%. It was estimated that there was an average of 159.9 Angiopep-2 molecules conjugated on each PS surface, provided that the density of PEG-PCL was 1.1 g/cm.[3,34]

PS permeability

As shown in Figure 2A, the fluorescence excitation spectra of HPTS were obviously pH dependent. The ratios of I_{454}/I_{403} and I_{403}/I_{454} vs pH value were regressed with the Boltzmann function (Figure 2B), and the correlativity of I_{454}/I_{403} and I_{403}/I_{454} vs pH was as follows:

I_{454}/I_{403} vs pH:

$$y = \frac{3.51562 + (0.01709 - 3.51562)}{1 + \exp((x - 7.92072)/0.42672)},\ R^2 = 0.9998$$

I_{403}/I_{454} vs pH:

$$y = \frac{0.08107 + (223.18529 - 0.08107)}{1 + \exp((x - 4.66866)/0.5238)},\ R^2 = 0.9999$$

Within the range of pH value from 6.0 to 10.0, the pH value and proton concentration in the external aqueous phase could be calculated according to the correlativity. The proton concentration vs the square root of diffusion time is plotted in Figure 2C, which shows a good linear relationship with different dioxane content. The slopes of these lines represent corresponding diffusion coefficients (D^*) of the protons with different dioxane content, and the value of D^* increases with

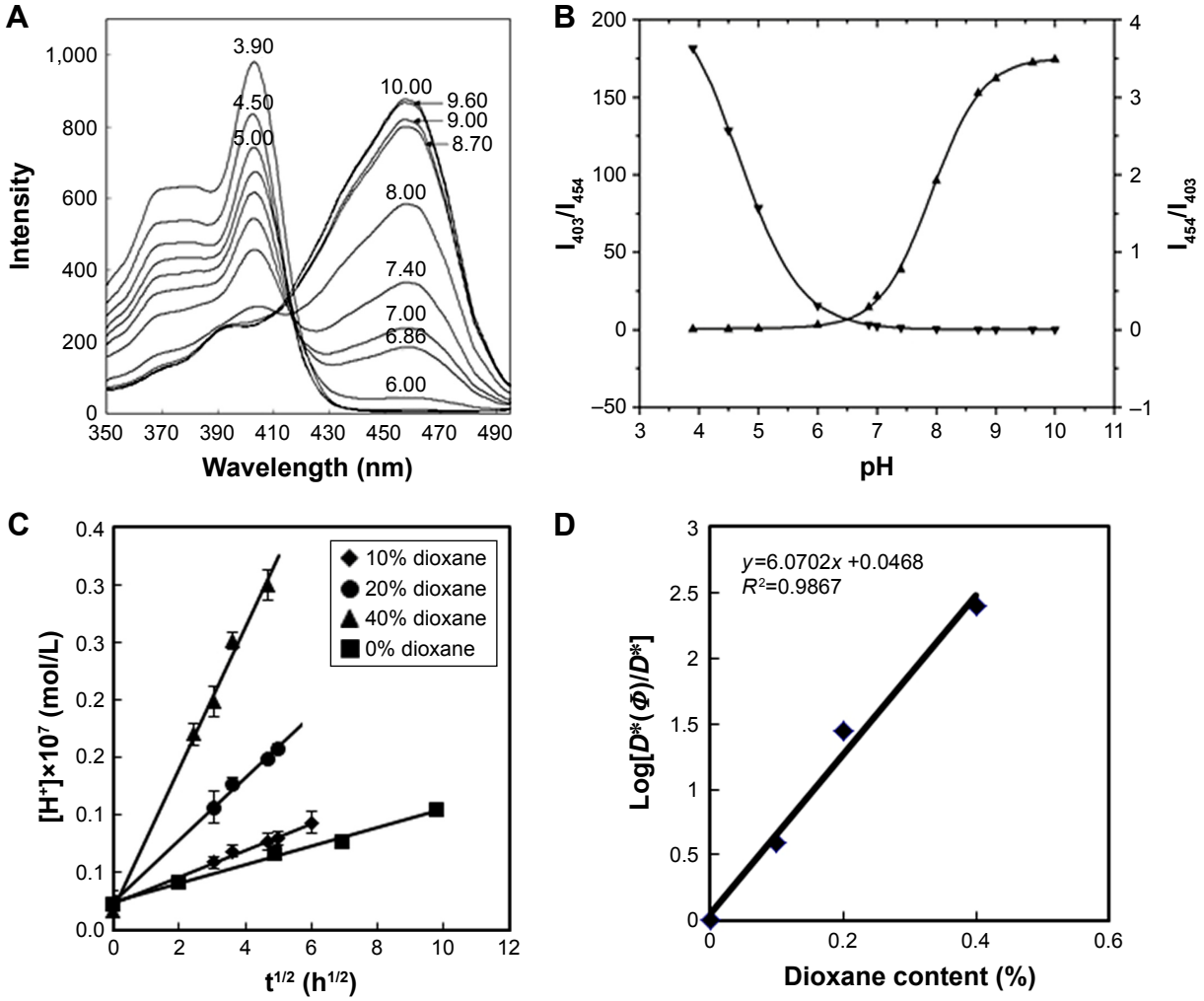

Figure 2 Proton permeability of polymersomes.

Notes: (**A**) Excitation spectra of HPTS in buffers with different pH values (Ex =509 nm). (**B**) Calibration profiles of HPTS, I_{454}/I_{403} or I_{403}/I_{454} vs pH were plotted and fitted with the Boltzmann function. (**C**) Plots of proton concentration [H^+] against the square root of diffusion time t. (**D**) Plot of log[$D^*(\Phi)/D^*(0\%)$] against dioxane content.

the dioxane content. Compared with liposomes, the D^* value of PS without dioxane is 5.93×10^{-23} cm^2/s, which is only 4.5% of that of liposomes (1.33×10^{-21} cm^2/s). These results suggest that PS are much less permeable than liposomes, indicating that drug-loaded PS might have good storage stability.

The curve of log[$D^*(\Phi)/D^*(0\%)$] against dioxane content is plotted in Figure 2D, where $D^*(\Phi)$ is the proton diffusion coefficient after the addition of dioxane and $D^*(0\%)$ is the proton diffusion coefficient without dioxane. The plot also displays a good linearity, which indicates that the permeability of PEG-PCL PS membrane could be precisely adjusted by the dioxane content outside the PS. The function of dioxane on PEG-PCL PS membrane permeability could be used to overcome the weak membrane permeability of PS during the active drug-loading process.

As shown in Table 1, by the means of active loading method, the DLC and EE for PS-DOX were 8.03%±0.16% and 96.1%±1.5%, respectively. The EE was much higher than those of other DOX-loaded PS (typically ranging between 10% and 15%) by the film rehydration method.[41] The DLC and EE for Ang-PS-DOX were 7.94%±0.17% and 95.0%±1.6%, respectively, indicating that the Angiopep-2 conjugation had no effect on PS DLC. After DOX loading, the size of PS-DOX and Ang-PS-DOX slightly increased to 125.6±13.5 and 135.2±18.1 nm, respectively. However, after DOX loading, the corresponding zeta potentials of PS-DOX and Ang-PS-DOX increased to −11.2±0.9 and −9±1.1 mV.

In vitro cumulative release

In vitro cumulative release of DOX from Ang-PS-DOX in different media was analyzed by a dialysis method. As shown in Figure 3, the cumulative 24 h release of DOX from Ang-PS-DOX in 10% plasma was higher than that in PBS, and the cumulative DOX release in pH 4.0 PBS was higher than that in pH 7.4 PBS. The media-related release profiles indicated that plasma protein, enzymes, and an acidic environment could promote DOX release from PS. In addition, during the first 8 h, the cumulative release of DOX was <30%, which indicates that DOX entrapped in Ang-PS might be mostly released in the tumor sites following the uptake of Ang-PS-DOX by brain.

Table 1 Characterization of DOX-loaded PS (n=4 per group)

Group	DLC (%)	EE (%)	Size (nm)	Zeta (mV)
PS-DOX	8.03±0.16	96.1±1.5	125.6±13.5	−11.2±0.9
Ang-PS-DOX	7.94±0.17	95.0±1.6	135.2±18.1	−9.8±1.1

Abbreviations: Ang-PS-DOX, Angiopep-2-conjugated biodegradable polymersomes loaded with doxorubicin; DLC, drug-loading capacity; DOX, doxorubicin; EE, encapsulation efficiency; PS, polymersomes.

Cellular uptake of Ang-PS-DOX

DOX inhibits tumor formation and development by intercalating in DNA fragments of tumor cells and hindering DNA transcription and replication.[24] Given this, abundant DOX uptake by the tumor cells is a prerequisite for effective therapy. As shown in Figure 3A, after 1 h incubation, Ang-PS-DOX showed greater accumulation in C6 cells than PS-DOX and DOX solution. Free DOX diffusing into the cells was mainly concentrated in the nuclei, while DOX-loaded PS were mostly distributed in the cytoplasm, which is consistent with the results of our previous work.[38] Flow cytometry results demonstrated that Ang-PS-DOX cellular uptake was ~3.3-fold that of PS-DOX (Figure 3B).

In vitro cytotoxicity of Ang-PS-DOX

As shown in Figure 3D, the cytotoxicity of DOX-loaded PS was concentration dependent. The IC_{50} values of DOX, PS-DOX, and Ang-PS-DOX were 2.9, 14.3, and 3.2 μg/mL, respectively, suggesting that the tumor cell-inhibiting effect of Ang-PS-DOX was increased by ~4.5-fold compared with that of PS-DOX. The abundant cytoplasmic uptake of Ang-PS-DOX into C6 cells mentioned above might be one important factor underlying the enhanced inhibition.

Pharmacokinetics and brain delivery of DOX-loaded PS

As shown in Figure 4A, the three DOX formulations were cleared in a biexponential manner. For the free DOX group, the plasma DOX concentration fell sharply to <0.1%ID/mL within 15 min, which was significantly lower than those of PS-DOX and Ang-PS-DOX. However, the plasma DOX concentrations for the PS-DOX and Ang-PS-DOX groups decreased slowly and remained around 0.1%ID/mL, 24 h after administration. These results indicated that DOX encapsulation in PS effectively decreased the plasma clearance of DOX. The pharmacokinetics parameters calculated from Figure 4A are shown in Table 2. The Cl value of free DOX was 585-fold and 492-fold that of PS-DOX and Ang-PS-DOX, respectively. The AUC_{0-t} and MRT_{0-t} of PS-DOX and Ang-PS-DOX were significantly higher than those of free DOX. There were significant differences in Cl, AUC_{0-t}, and MRT_{0-t} between PS-DOX and Ang-PS-DOX ($P<0.05$), indicating that Angiopep-2 modification of PS significantly increased PS blood clearance. The results might be related to extensive LRP1 expression in other organs (eg, liver) and cells (eg, vascular smooth muscle cells, neurons, macrophages, and fibroblasts).[42]

At 24 h after i.v. injection of different DOX formulations in C6 glioma-transplanted rats, DOX uptake rates in the

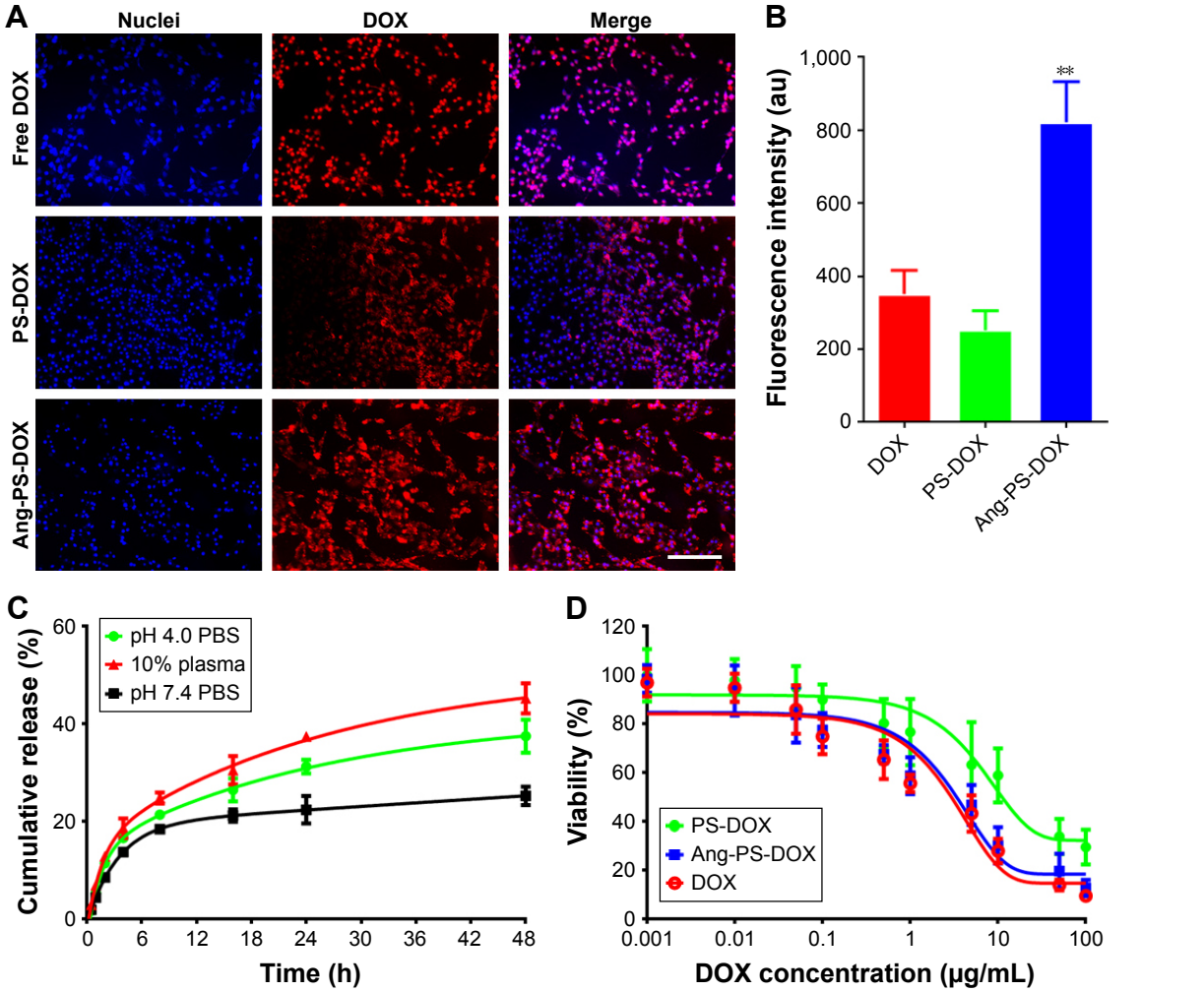

Figure 3 Ang-PS-DOX characterization.

Notes: (**A**) Cellular uptake of doxorubicin (DOX)-loaded PS. Bar =500 μm. (**B**) Mean fluorescence intensity of DOX per cell. (**C**) Cumulative release (%) of DOX from Ang-PS-DOX in different media. (**D**) C6 viability inhibition-logarithmic DOX concentration curves of DOX-loaded PS. $^{**}P<0.01$ vs PS-DOX.

Abbreviations: Ags-PS-DOX, Angiopep-2-conjugated biodegradable polymersomes loaded with doxorubicin; au, arbitrary unit; PBS, phosphate-buffered saline; PS, polymersomes.

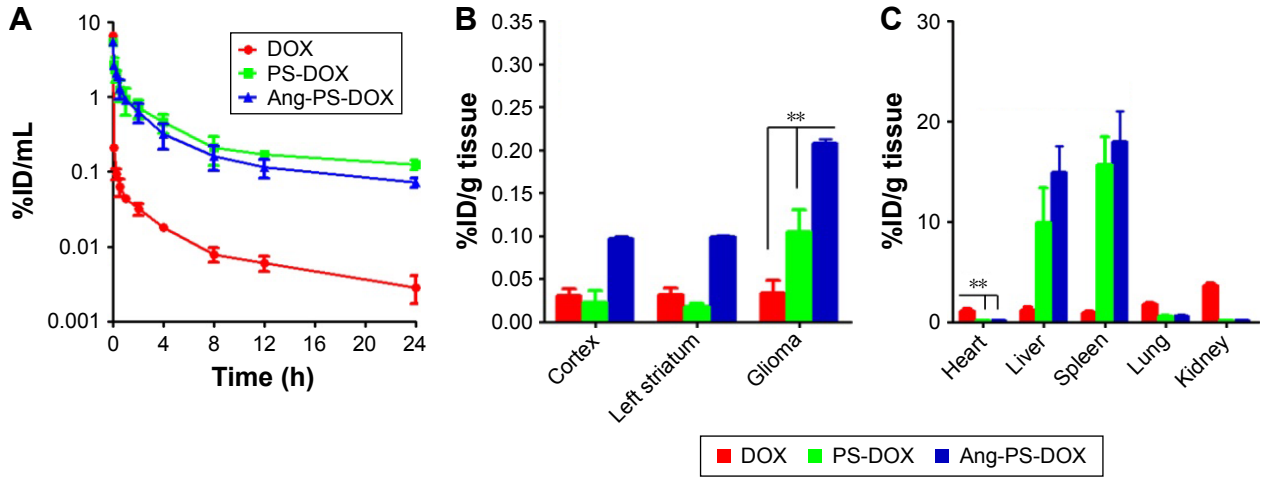

Figure 4 Ang-PS-DOX pharmacokinetics and brain tumor delivery.

Notes: (**A**) %ID/mL of doxorubicin (DOX) in the plasma was plotted vs time after i.v. injection of DOX solution (PS-DOX or Ang-PS-DOX) in C6-glioma-bearing rats at the DOX dose of 5 mg/kg. (**B**) DOX uptake in the brain tissues 24 h post i.v. injection; $^{**}P<0.01$ vs Ang-PS-DOX. (**C**) Biodistribution of DOX in major organs 24 h after i.v. injection; $^{**}P<0.01$ vs DOX. Data represent mean ± standard deviation (n=6).

Abbreviations: Ang-PS-DOX, Angiopep-2-conjugated biodegradable polymersomes loaded with doxorubicin; %ID, injected dose; i.v., intravenous.

Table 2 Pharmacokinetics parameters of DOX-loaded PS in plasma (n=4 per group)

Group	AUC_{0-t} (%ID h/mL)	Cl (L/h)	MRT_{0-t} (h)
DOX	0.52±0.06	1,890±208	1.49±0.18
PS-DOX	5.73±0.58[a]	3.23±0.33[a]	5.41±0.56[a]
Ang-PS-DOX	4.96±0.47[a,b]	3.84±0.32[a,b]	4.30±0.36[a,b]

Notes: [a]$P<0.01$ vs DOX, [b]$P<0.05$ vs PS-DOX group.
Abbreviations: Ang-PS-DOX, Angiopep-2-conjugated biodegradable polymersomes loaded with doxorubicin; AUC_{0-t}, area under the concentration–time curve; Cl, clearance; DOX, doxorubicin; %ID, percentage of injected dose; MRT, mean residence time; PS, polymersomes.

cortex, left striatum, and glioma tumors were quantitatively analyzed to investigate the brain tumor delivery property of Ang-PS-DOX. As shown in Figure 4B, for the free DOX group, there was no significant difference in DOX uptake among different brain tissues. For the PS-DOX group, DOX uptake rates in the cortex and left striatum were slightly lower than that for the free DOX group, but it was increased notably in the glioma tissue. The finding might be attributable to the weak EPR effect of glioma and the long circulatory time of PS-DOX. For the Ang-PS-DOX group, DOX uptake in the brain tissue, especially in the glioma tumors (0.21%/g), was significantly higher than that for free DOX (0.03%/g) and PS-DOX (0.11%/g). These results suggest that Angiopep-2 conjugation with PS could significantly improve brain delivery, and Ang-PS might be a promising carrier for brain drug delivery, especially for glioma tumors. DOX distribution in other tissues revealed that DOX-loaded PS accumulated mostly in the spleen and liver; this was slightly increased by Angiopep-2 modification (Figure 4C). Compared with free DOX, DOX-PS and Ang-PS-DOX showed significantly lower DOX accumulation in the heart, suggesting that PS might have the potential to decrease DOX-associated cardiotoxicity.

In vivo distribution of Ang-PS-DOX in glioma tissues

In vivo distribution of PS-DOX and Ang-PS-DOX in glioma, 24 h after i.v. administration, was investigated by fluorescence imaging. As shown in Figure 5, the distribution of Ang-PS-DOX in glioma was more extensive than that of PS-DOX. Moreover, compared with PS-DOX, more Ang-PS-DOX or DOX entered the cytoplasm or even the nuclei of tumor cells, which might facilitate the tumor inhibition ability of DOX. The distribution pattern of Ang-PS-DOX might be due to active BBB and glioma targeting by LRP1-mediated endocytosis.[18]

In vivo antiglioma efficacy

After four cycles of drug administration, the survival times of glioma-bearing rats were monitored to evaluate the antiglioma efficacy of Ang-PS-DOX. The life spans of glioma-bearing rats treated with free DOX solution, PS-DOX, Ang-PS-DOX, or saline are shown in Figure 6A and Table 3. The median survival times were 15, 19, 22, and 32 days, respectively. For the PS-DOX group, the survival time of glioma-bearing rats was 46.7% longer compared to the control group ($P<0.05$) and 15.8% longer than the DOX solution group. For the Ang-PS-DOX group, the survival time was increased by 113% ($P<0.01$) and 15.8% ($P<0.05$) compared with those of the control and DOX solution groups, respectively. Moreover, compared with PS-DOX, Ang-PS-DOX significantly further prolonged the survival time of glioma-bearing rats ($P<0.05$). This was presumably due to its active targeting property by LRP1-mediated endocytosis, long circulatory half-life, and the EPR effect. Body weight changes in different groups could be used to evaluate the

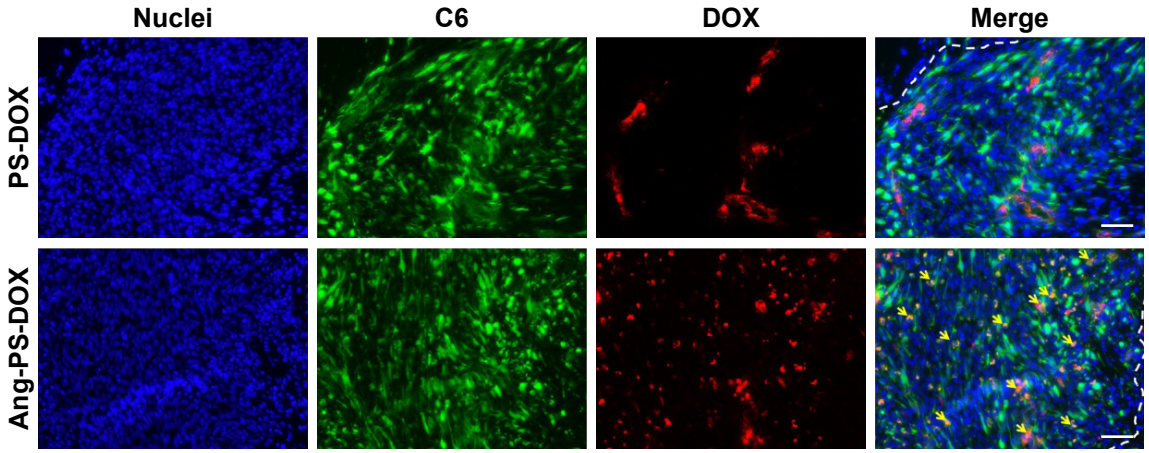

Figure 5 Glioma distribution of Ang-PS-DOX.
Notes: Blue, cell nuclei; green, C6 cells expressing green fluorescent protein; red, DOX. Yellow arrows in the merged images indicate the overlay of PS and C6 cells; white dotted lines indicate the edges of glioma tumors. Bar=250 μm. The magnification is 200.
Abbreviations: Ang-PS-DOX, Angiopep-2-conjugated biodegradable polymersomes loaded with doxorubicin; DOX, doxorubicin; PS, polymersomes.

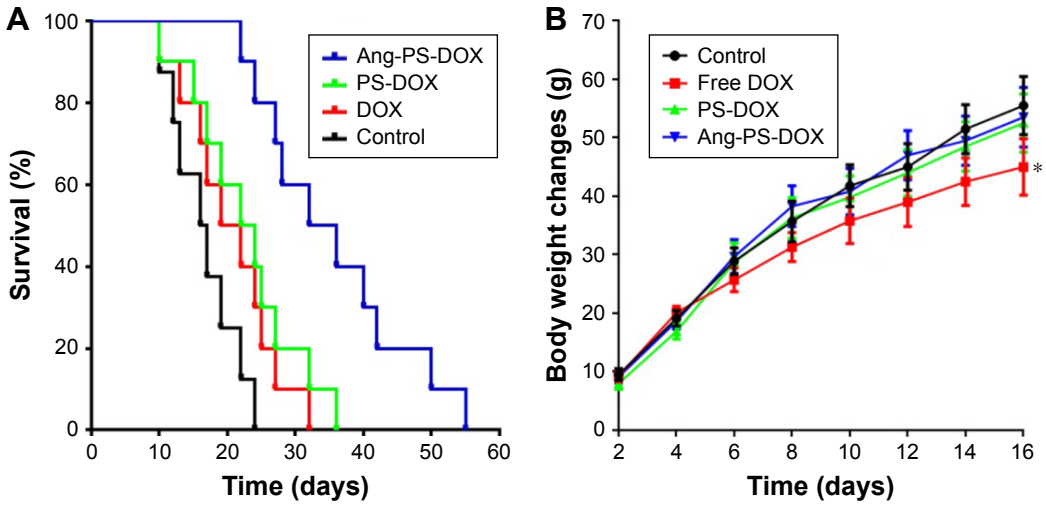

Figure 6 Antiglioma efficacy of Ang-PS-DOX.
Notes: (**A**) Survival (Kaplan–Meier plots) of C6 glioma rat models after Ang-PS-DOX treatment (n=10). (**B**) Body weight changes of C6 glioma rat models after Ang-PS-DOX treatment (n=10). *$P<0.05$ vs control.
Abbreviations: Ang-PS-DOX, Angiopep-2-conjugated biodegradable polymersomes loaded with doxorubicin; DOX, doxorubicin.

side effects of different treatments. As shown in Figure 6B, compared with saline, different DOX formulations, except free DOX, did not significantly decrease the body weight, indicating that Ang-PS-DOX might be a safe treatment. These promising results demonstrate the enormous potential of Ang-PS-DOX in clinical glioma therapy.

Conclusion

In the present study, we developed a dual-targeting brain tumor drug delivery system, Angiopep-2-conjugated PS loaded with DOX. The PEG-PCL PS were prepared by a film hydration method. The proton permeability of the PS membrane was much less than that of liposomes, and it could be adjusted by dioxane. In vitro cellular uptake and MTT assays demonstrated Ang-PS-DOX gathered more in C6 cells and lowered the IC_{50} to a greater extent than PS-DOX. In vivo brain delivery and glioma slice imaging revealed that Ang-PS-DOX demonstrated stronger accumulation in the glioma tissue and higher tumor cell uptake than PS-DOX. Moreover, Ang-PS-DOX significantly improved the survival time of glioma-bearing rats, compared to free DOX solution and PS-DOX. These promising results indicate that Ang-PS-DOX might have great potential in brain tumor therapy.

Table 3 Median survival times for glioma-implanted rats (n=10 per group)

Group	Median (days)	Standard error	95% confidence interval	Log-rank test	ISTc	ISTs
Control	15	1.6	11.9–18.1	–	–	–
Free DOX	19	4.0	11.3–26.7		26.7	–
PS-DOX	22	4.0	14.3–29.7	[a]	46.7	15.8
Ang-PS-DOX	32	6.3	19.6–44.4	[b,c,d]	113	68.4

Notes: Dosage of DOX is 4×1.5 mg/kg. Log-rank test. [a]$P<0.05$, [b]$P<0.01$ vs control, [c]$P<0.01$ vs free DOX, [d]$P<0.05$ Ang-PS-DOX vs PS-DOX. The increases in survival times (%) are compared to control (ISTc) or DOX solution (ISTs).
Abbreviations: Ang-PS-DOX, Angiopep-2-conjugated biodegradable polymersomes loaded with doxorubicin; DOX, doxorubicin.

Acknowledgments

The present study was supported by the National Basic Research Program of China (973 Program, 2013CB932502), the National Natural Science Foundation of China (81472757, 81361140344), and doctoral fund of the Ministry of Education of China (20100071120050).

Disclosure

The authors report no conflicts of interest in this work.

References

1. Ostrom QT, Bauchet L, Davis FG, et al. The epidemiology of glioma in adults: a "state of the science" review. *Neuro Oncol*. 2014;17(4):896–913.
2. Wrensch M, Fisher JL, Schwartzbaum JA, Bondy M, Berger M, Aldape KD. The molecular epidemiology of gliomas in adults. *Neurosurg Focus*. 2005;19(5):E5.
3. Stupp R, Mason WP, Van den Bent MJ, et al. Radiotherapy plus concomitant and adjuvant temozolomide for glioblastoma. *N Engl J Med*. 2005;352(10):987–996.
4. Stupp R, Hegi ME, Mason WP, et al. Effects of radiotherapy with concomitant and adjuvant temozolomide versus radiotherapy alone on survival in glioblastoma in a randomised phase III study: 5-year analysis of the EORTC-NCIC trial. *Lancet Oncol*. 2009;10(5):459–466.
5. Ong BYS, Ranganath SH, Lai YL, et al. Paclitaxel delivery from PLGA foams for controlled release in post-surgical chemotherapy against glioblastoma multiforme. *Biomaterials*. 2009;30(18):3189–3196.
6. Pardridge WM. Blood–brain barrier delivery. *Drug Discov Today*. 2007;12(1–2):54–61.
7. Minchinton AI, Tannock IF. Drug penetration in solid tumours. *Nat Rev Cancer*. 2006;6(8):583–592.

8. Burkhardt JK, Riina H, Shin BJ, et al. Intra-arterial delivery of bevacizumab after blood-brain barrier disruption for the treatment of recurrent glioblastoma: progression-free survival and overall survival. *World Neurosurg*. 2012;77(1):130–134.
9. Warren K, Jakacki R, Widemann B, et al. Phase II trial of intravenous lobradimil and carboplatin in childhood brain tumors: a report from the Children's Oncology Group. *Cancer Chemother Pharmacol*. 2006; 58(3):343–347.
10. Lin F, de Gooijer MC, Hanekamp D, Brandsma D, Beijnen JH, van Tellingen O. Targeting core (mutated) pathways of high-grade gliomas: challenges of intrinsic resistance and drug efflux. *Cns Oncol*. 2015; 2(3):271–288.
11. Ché C, Yang G, Thiot C, et al. New angiopep-modified doxorubicin (ANG1007) and etoposide (ANG1009) chemotherapeutics with increased brain penetration. *J Med Chem*. 2010;53(7):2814–2824.
12. Gaillard PJ, Kerklaan BM, Aftimos P, et al. Abstract CT216: phase I dose escalating study of 2B3-101, glutathione PEGylated liposomal doxorubicin, in patients with solid tumors and brain metastases or recurrent malignant glioma. *Cancer Res*. 2014;74(19):CT216–CT216.
13. Barua NU, Gill SS, Love S. Convection-enhanced drug delivery to the brain: therapeutic potential and neuropathological considerations. *Brain Pathol*. 2014;24(2):117–127.
14. Gabathuler R. Approaches to transport therapeutic drugs across the blood–brain barrier to treat brain diseases. *Neurobiol Dis*. 2009;37(1):48–57.
15. Méresse S, Delbart C, Fruchart JC, Cecchelli R. Low-density lipoprotein receptor on endothelium of brain capillaries. *J Neurochem*. 1989; 53(2):340–345.
16. Dehouck B, Dehouck MP, Fruchart JC, Cecchelli R. Upregulation of the low density lipoprotein receptor at the blood-brain barrier: intercommunications between brain capillary endothelial cells and astrocytes. *J Cell Biol*. 1994;126(2):465–473.
17. Pardridge WM. Molecular biology of the blood-brain barrier. *Mol Biotechnol*. 2005;30(1):57–70.
18. Demeule M, Currie JC, Bertrand Y, et al. Involvement of the low-density lipoprotein receptor-related protein in the transcytosis of the brain delivery vector angiopep-2. *J Neurochem*. 2008;106(4):1534–1544.
19. Miida T, Hirayama S. Lipoproteins and their receptors in the central nervous system. *Rinsho Byori*. 2009;57(1):48–53.
20. Hussain MM, Strickland DK, Bakillah A. The mammalian low-density lipoprotein receptor family. *Annu Rev Nutr*. 1999;19:141–172.
21. Jiang W, Xie H, Ghoorah D, et al. Conjugation of functionalized SPIONs with transferrin for targeting and imaging brain glial tumors in rat model. *Plos One*. 2012;7(5):e3737.
22. Huang R, Ke W, Han L, et al. Lactoferrin-modified nanoparticles could mediate efficient gene delivery to the brain in vivo. *Brain Res Bull*. 2010; 81(6):600–604.
23. Zhou QH, Lu JZ, Hui KW, Boado RJ, Pardridge WM. Delivery of a peptide radiopharmaceutical to brain with an IgG-avidin fusion protein. *Bioconjug Chem*. 2011;22(8):1611–1618.
24. Lei H, Wang X, Wu C. Early stage intercalation of doxorubicin to DNA fragments observed in molecular dynamics binding simulations. *J Mol Graph Model*. 2012;38:279–289.
25. Zhang Y, Yu J, Zhang L, Cai J, Cai D, Lv C. Enhanced anti-tumor effects of doxorubicin on glioma by entrapping in polybutylcyanoacrylate nanoparticles. *Tumour Biol*. 2015:37(2):2703–2708.
26. Discher DE, Ahmed F. Polymersomes. *Annu Rev Biomed Eng*. 2006; 8:323–341.
27. Zhao L, Li N, Wang K, Shi C, Zhang L, Luan Y. A review of polypeptide-based polymersomes. *Biomaterials*. 2014;35(4):1284–1301.
28. Yuan M, Wang Y, Li X, et al. Polymerization of lactides and lactones. 10. synthesis, characterization, and application of amino-terminated poly(ethylene glycol)-co-poly(ε-caprolactone) block copolymer. *Macromolecules*. 2000;33(5):1613–1617.
29. Abraham SA, Edwards K, Karlsson G, Hudon N, Mayer LD, Bally MB. An evaluation of transmembrane ion gradient-mediated encapsulation of topotecan within liposomes. *J Control Release*. 2004;96(3):449–461.
30. Choucair A, Soo PL, Eisenberg A. Active loading and tunable release of doxorubicin from block copolymer vesicles. *Langmuir*. 2005;21(20): 9308–9313.
31. Wu J, Eisenberg A. Proton diffusion across membranes of vesicles of poly(styrene-b-acrylic acid) diblock copolymers. *J Am Chem Soc*. 2006; 128(9):2880–2884.
32. Olivier JC, Huertas R, Lee HJ, et al. Synthesis of pegylated immunonanoparticles. *Pharm Res*. 2002;19(8):1137–1143.
33. Sun X, Pang Z, Ye H, et al. Co-delivery of pEGFP-hTRAIL and paclitaxel to brain glioma mediated by an angiopep-conjugated liposome. *Biomaterials*. 2011;33(3):916–924.
34. Pang Z, Lu W, Gao H, et al. Preparation and brain delivery property of biodegradable polymersomes conjugated with OX26. *J Control Release*. 2008;128(2):120–127.
35. Flaten GE, Bunjes H, Luthman K, et al. Drug permeability across a phospholipid vesicle-based barrier: 2. Characterization of barrier structure, storage stability and stability towards pH changes *Eur J Pharm Sci*. 2006;28(4):336–343.
36. Heerklotz H, Seelig J. Leakage and lysis of lipid membranes induced by the lipopeptide surfactin. *Eur Biophys J*. 2007;36(4–5):305–314.
37. Yu Y, Pang Z, Lu W, et al. Self-assembled polymersomes conjugated with lactoferrin as novel drug carrier for brain delivery. *Pharm Res*. 2012; 29(1):83–96.
38. Pang Z, Gao H, Yu Y, et al. Enhanced intracellular delivery and chemotherapy for glioma rats by transferrin-conjugated biodegradable polymersomes loaded with doxorubicin. *Bioconjug Chem*. 2011;22(6): 1171–1180.
39. Pang Z, Feng L, Hua R, et al. Lactoferrin-conjugated biodegradable polymersome holding doxorubicin and tetrandrine for chemotherapy of glioma rats. *Mol Pharm*. 2010;7(6):1995–2005.
40. Huwyler J, Wu D, Pardridge WM. Brain drug delivery of small molecules using immunoliposomes. *Proc Natl Acad Sci U S A*. 1996; 93(24):14164–14169.
41. Figueiredo P, Balasubramanian V, Shahbazi MA, et al. Angiopep2-functionalized polymersomes for targeted doxorubicin delivery to glioblastoma cells. *Int J Pharm*. 2016;511(2):794–803.
42. Strickland DK, Au DT, Cunfer P, Muratoglu SC. Low-density lipoprotein receptor-related protein-1: role in the regulation of vascular integrity. *Arterioscler Thromb Vasc Biol*. 2014;34(3):487–498.